Available online at www.sciencedirect.com

ScienceDirect

Procedia Structural Integrity 58 (2024) 30–34

Structural Integrity Procedia

www.elsevier.com/locate/procedia

7th International Conference on Structural Integrity and Durability (ICSID 2023)

Compression behavior of diamond cellular structure made of Inconel 718

Katarina Monkova[a,b]*, George Pantazopoulos[c]†, Peter Pavol Monka[a,b], Anagnostis Toulfatzis[c], Peter Baron[a], Sofia Papadopoulou[c]

[a]*Faculty of Manufacturing Technologies, Technical University in Kosice, Sturova 31, 080 01 Presov, Slovakia*
[b]*Faculty of Technology, Tomas Bata University in Zlin, Nam. T.G. Masaryka 275, 760 01 Zlin, Czech*
[c]*ELKEME Hellenic Research Centre for Metals S.A., 61st km Athens—Lamia National Road, 32011 Oinofyta, Greece*

Abstract

The article aims to investigate compression behaviour of Diamond cellular structure at different cross-head speeds. The samples were made of Inconel 718 alloy by DMLS (Direct Metal Laser Sintering) technology and heat treated according to AMS 5664 procedure. The compression tests were performed according to ASTM E9 international standard at ambient temperature employing a servohydraulic testing machine Instron 8802 with a maximum capacity of 250 kN at three different cross-head speeds v = 1; 10 and 100 mm/min. The results showed that testing speed does not affect significantly the maximum force results, and that the Diamond structure of 20 % volume fraction exceeded the upper load limit of the testing machine, i.e. 250 kN, for all three testing speeds.

Keywords: compression; Inconel 718; additive manufacturing; cellular structure; diamond, cross-head speed.

1. Introduction

Lightweight structure plays a crucial role in the development of green products. For instance, in the design of new-generation transportation systems, lightweight structures help reducing fuel costs and allow vehicles to achieve

* Corresponding authors. Tel.: +421 55 602 6370.
E-mail address: katarina.monkova@tuke.sk
†Corresponding authors. Tel.: +30-2262-60-4463
E-mail address: gpantaz@elkeme.vionet.gr

10.1016/j.prostr.2024.05.006

improved performance. (Gibson et al., 2010; Petrova & Schmauder, 2020) Moreover, lightweight designs are important in biomedical applications, including implant and scaffold designs. The development of engineering materials to achieve lightweight and multifunctional structures is of increasing interest, aided by the development of advanced fabrication processes, including additive manufacturing. (Infante, et al., 2019; Sahraoui et al., 2020)

The properties of cellular lightweight bodies are the result of a combination of the properties of the cellular structure and the properties of the material used for its production. These two factors together with the volume fraction of the cell bodies that is given by equation (1): (Monkova et al., 2023)

$$V_f = (material\ volume)/(total\ sample\ volume) \tag{1}$$

are the determining parameters for their physical and mechanical properties.

2. Materials and methods

In this study, the behavior of the Diamond structures with a basic cell of 10 x 10 x 10 mm, total sizes of the samples 40 x 40 x 50 mm and three various volume fractions (V_f = 10; 15 and 20 %) were studied during compression tests.

Diamond belongs to the so-called Triply Periodic Minimal Surfaces (TPMS). A minimal surface can be defined as a surface on which, at each point, the two principal curvatures are equal in value but have opposite signs (i.e., there is a mean curvature of zero value at all points) (Cosma et al., 2020; Yong et al., 2020). TPMS structures can be mathematically modelled using level-set equations. For the Diamond structure, the equation is as follows (Psihoyos et al., 2021):

$$\sin(x)\sin(y)\sin(z) + \sin(x)\cos(y)\cos(z) + \cos(x)\sin(y)\cos(z) + \cos(x)\cos(y)\sin(z) = 0 \tag{2}$$

A basic cell of the Diamond structure used for the research is presented in Fig. 1a, while virtual 3D model of the compression samples prepared in software PTC Creo 8 is shown in Fig. 1b.

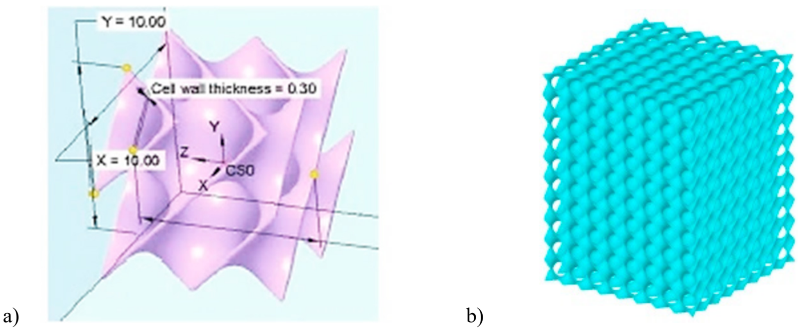

Fig. 1. Diamond structure a) basic cell; b) virtual 3D model of the sample with 10 % volume fraction.

3D-printed Inconel 718 cellular specimens were manufactured by Direct Laser Metal Sintering (DLMS) technology employing EOS EOSINT M290 and they were heat treated by procedure AMS 5664 according to EOS Inconel 718 datasheet (Mikula et al., 2021).

Inconel 718 is a well-known, nickel chromium workhorse material for the additive manufacturing industry. The material is composed mainly of 50-55 %wt. Ni, 17-21 %wt. Cr, 4.75-5.5 % Nb, 2.8-3.3 % wt. Mo, 0.65-1.15 %wt. Ti, 0.20-0.80 %wt. Al and Fe as a balance (EOS Nickel Alloy IN 718, 2014). It is characterised by stability in extreme environments and ability to remain resistant to corrosion, creep, and thermal shock. This nickel superalloy has an intrinsic ability to create a strong and stable oxide layer when exposed to heat (Moreira et al., 2020; Mlikota et al., 2021). The natural passivation feature protects the material against damage. Because of its unique properties, Inconel 718 has become useful in a wide range of applications ranging from manufacturing operations to military equipment and the aerospace industry (Ferro et al., 2023; Kastratović et al., 2021; Khosravani et al., 2021).

The compression tests (Fig. 2) were performed according to ASTM E9 international standard (ASTM E9 Standard, 2019) at ambient temperature employing a servohydraulic testing machine Instron 8802 with a maximum capacity of 250 kN at three different cross-head speeds (v = 1; 10 and 100 mm/min).

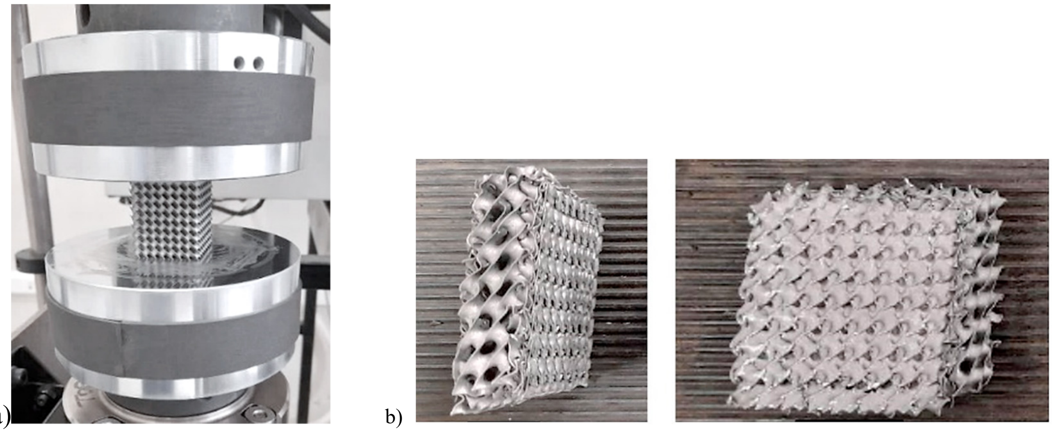

a) b)

Fig. 2. a) Compressive testing set-up; b) a sample V_f = 15 % after compression at a cross-head speed of 10 mm/min.

3. Results and discussion

Measured force load dependences on displacement for all three cross-head speeds of 1; 10 and 100 mm/min are displayed in Fig. 3, and the results obtained for all investigated samples are plotted in histogram in Fig. 4.

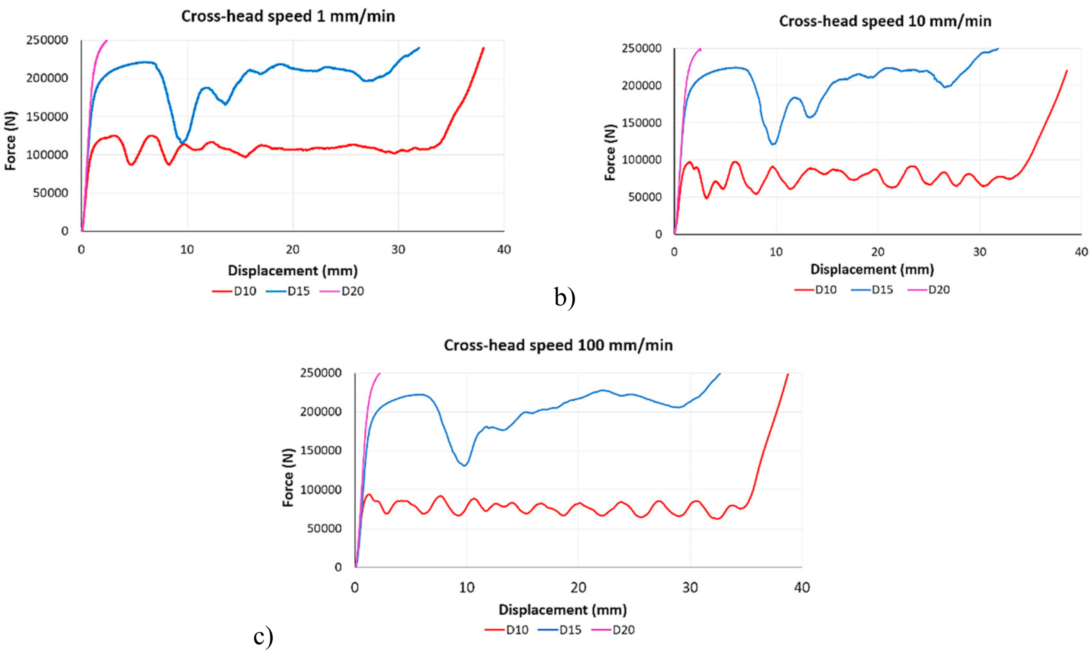

a) b) c)

Fig. 3. Indicative compressive force-displacement curves at a cross-head speed: a) 1 mm/min; b) 10 mm/min, c) 100 mm/min.

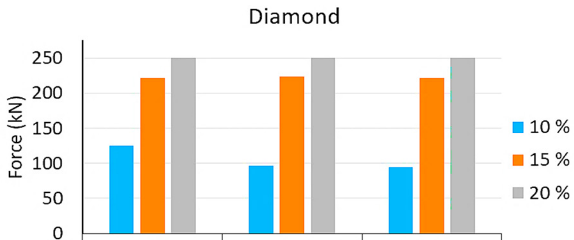

	1	10	100
10 %	125	97	94
15 %	221	224	222
20 %	250	250	250

Cross-head speed (mm/min)

Fig. 4. Maximum forces measured at different testing speed and volume fractions (limited by testing machine capacity 250 kN).

Already measured dependences of force on elongation indicated differences in the behaviour of individual structures under pressure loading, not only in the maximum force, but also in displacement and so in energy-absorption capabilities. For the Diamond structure, it was not possible to determine the exact value of the maximum force, as the capacity of the testing machine was not sufficient, but it can be clearly stated that this structure appears to be the most resistant to compressive loading at all three crossbar speeds. In all three tests (at all three traverse speeds), the oscillations in the measured dependences were probably related to the damages. After the first peak, the force decreased until the structure could not interact with the next layer of intact cells, leading to an increase in force. The number of these load alterations corresponded to the number of interactions within individual cell layers (Alexopoulou et al., 2022; Niutta et al., 2022).

4. Conclusions

Lightening components and devices is currently a trend that brings many benefits. When applying cellular structures, knowledge of their behaviour in different conditions is a prerequisite for their correct and appropriate implementation. This study was aimed at determining the properties of the Diamond-type structure, which was prepared by DMLS technology in three different volume fractions and tested under compressive loading at three different crosshead speeds.

The results showed that the increase of the volume ratio induces an augmentation of the maximum compressive load at the first peak but testing speed does not affect significantly the maximum force results, especially for 15 % volume ratio (variations <5%). The Diamond structure of 20 % volume ratio exceeded the upper load limit of the testing machine, i.e. 250 kN, for all three testing speeds.

Acknowledgements

The article was prepared thanks to support of the Ministry of Education of the Slovak Republic through the grants APVV-19-0550, KEGA 005TUKE-4/2021 and KEGA 032TUKE-4/2022.

References

Alexopoulou, V.E., Papazoglou, E.L., Karmiris-Obratański, P., Markopoulos, A.P., 2022. 3D finite element modeling of selective laser melting for conduction, transition and keyhole modes. Journal of Manufacturing Processes 75, 877–894.

ASTM E9:2019. Standard Test Methods of Compression Testing of Metallic Materials at Room Temperature, ASTM International, United States.

Cosma, C., Drstvensek, I., Berce, P. et al., 2020. Physical-Mechanical Characteristics and Microstructure of Ti6Al7Nb Lattice Structures Manufactured by Selective Laser Melting. Materials 13, 18.

EOS Nickel Alloy IN 718, 2014, Material Data Sheet, EOS GmbH - Electro Optical Systems, TMS, WEIL / 05.2014

Ferro, P. et al., Creating IN718-High Carbon Steel bi-metallic parts by Fused Deposition Modeling and Sintering. Procedia Structural Integrity 47, 535-544.

Gibson, I., Rosen, D.W., Stucker, B., 2010. Additive manufacturing technologies: Rapid prototyping to direct digital manufacturing. New York: Springer.
Infante, V., Freitas, M., Fonte, M., 2019. Failure analysis of a crankshaft of a helicopter engine. Engineering Failure Analysis 100, 49–59.
Kastratović, G. et al., 2021.Composite material selection for aircraft structures based on experimental and numerical evaluation of mechanical properties. Procedia Structural Integrity 31, 127-133.
Khosravani, M. R., Reinicke, T., Fracture behavior of intact and defected 3D-printed parts, Procedia Structural Integrity, 31, 2021, 105-110.
Mikula, J., Ahluwalia R., Laskowski, R. et al., 2021. Modelling the influence of process parameters on precipitate formation in powder-bed fusion additive manufacturing of IN718. Materials & Design 207, 109851.
Mlikota, M., Schmauder, S., Dogahe, K., Božić, Ž., 2021. Influence of local residual stresses on fatigue crack initiation. Procedia Structural Integrity 31, 3-7.
Monkova, K. et al., 2023. Effect of Crosshead Speed and Volume Ratio on Compressive Mechanical Properties of Mono- and Double-Gyroid Structures Made of Inconel 718. Materials 16, 4973.
Moreira, M.F., Fantin, L.B., Beneduce Neto, F., Azevedo, C.R.F., 2020. Microstructural and mechanical characterization of as-cast nickel-based superalloy (IN-713C). International Journal of Metalcasting, 15, 1129–1148.
Niutta, C. B., et al., 2022. Defect-Driven topology optimization for fatigue design of additive manufacturing structures: Application on a real industrial aerospace component. Engineering Failure Analysis 142, 106737.
Petrova, V., Schmauder, S., 2020. Analysis of interacting cracks in functionally graded thermal barrier coatings. Procedia Structural Integrity 28, 608-618.
Psihoyos, H.O., Lampeas, G.N., Pantelakis, S.G., 2021. A modelling framework for fatigue-life prediction of selective laser melting additive manufactured Ti-6Al-4V. Procedia Structural Integrity 34, 253–258.
Sahraoui, Z.; Mehdi, K., Jaber, M.B., 2020. Analytical and experimental stability analysis of AU4G1 thin-walled tubular workpieces in turning process. Proceedings of the Institution of Mechanical Engineers, Part B: Journal of Engineering Manufacture 234, 1007–1018.
Yong, C.K., Gibbons, G.J., Wong, C.C., West. G., 2020. A Critical Review of the Material Characteristics of Additive Manufactured IN718 for High-Temperature Application. Metals 10, 12, 1576.